GEOPHYSICAL RESEARCH LETTERS, VOL. 33, L08602, doi:10.1029/2006GL025891, 2006

Decadal variability of the Indian Ocean cross-equatorial exchange in SODA

Rena Schoenefeldt[1] and Friedrich A. Schott[1]

Received 29 January 2006; revised 7 March 2006; accepted 13 March 2006; published 20 April 2006.

[1] The mean meridional circulation across the equator in the Indian Ocean is characterized by the shallow Cross-Equatorial Cell (CEC). At the western boundary, the Somali Current transports thermocline waters northward which then upwell, mostly off Northeast Africa. The upwelled waters are taking up heat and then exported back southward by southward near-surface Ekman and Sverdrup transports. The CEC is closed by subduction in the southeastern subtropics and includes contributions from the Indonesian Throughflow. In an analysis of output from the SODA assimilation, a decadal slowdown of the different branches of the CEC is demonstrated here. **Citation:** Schoenefeldt, R., and F. A. Schott (2006), Decadal variability of the Indian Ocean cross-equatorial exchange in SODA, *Geophys. Res. Lett.*, *33*, L08602, doi:10.1029/2006GL025891.

1. Introduction

[2] The meridional circulation of the Indian Ocean differs drastically from the Pacific and Atlantic because it does not have a northern subpolar regime. As a consequence, the heat gained in the northern Indian Ocean is exported southward across the equator. The main mechanism by which this heat transport is accomplished is the Cross-equatorial Cell (CEC) [*Schott et al.*, 2002; *Miyama et al.*, 2003]. The driving of the mean CEC is due to the dominance of the summer monsoon over the winter monsoon, leading to annual-mean southward Ekman transports in the northern hemisphere and south of the equator (Figure 1).

[3] As pointed out by *Godfrey et al.* [2001] and *Miyama et al.* [2003] there is an approximate equivalency of the mean Ekman and Sverdrup transports near the equator. The reason is the near-linear gradient of zonal wind stress across the equator which leads to a vanishing geostrophic divergence. Therefore the driver of the mean CEC is the Sverdrup transport, and indeed, an approximate balance has been found [*Schott et al.*, 2002] between the mean northward thermocline transports of the Somali Current and southward cross-equatorial export by the Sverdrup transport, yielding a mean CEC transport of $6 \cdot 10^6 m^3 s^{-1}$ (or Sverdrups = Sv).

[4] A further Indian Ocean peculiarity is given by the fact that right on the equator the winds are northward, mostly in the western basin and caused by the cross-equatorial Findlater Jet of the summer monsoon. As a consequence, northward surface currents occur on the equator, against the southward Ekman transports in both hemispheres. The result is a shallow equatorial roll, confined to the mixed layer, with the Ekman flow passing southward underneath the northward surface flow [*Wacongne and Pacanowski*, 1996; *Miyama et al.*, 2003].

[5] While the monsoon cycle of the Indian Ocean, including the cross-equatorial exchanges involved, is fairly well understood by now [*Schott and McCreary*, 2001], very little is known about the interannual and longer-term variability of the meridional circulation across the equator. For the southern hemispheric tropics, a decrease of Ekman divergence and upwelling at the northern edge of the Southeast Trades was reported by *Lee* [2004] for the recent decade of satellite scatterometer winds, and linked to observed south Indian Ocean warming. We investigate here the evidence for decadal variations of the cross-equatorial exchanges in output fields from the Simple Ocean Data Assimilation (SODA) model of *Carton et al.* [2000].

2. SODA Output

[6] The SODA product (named beta-7) is available at $1^\circ \times 1^\circ$ resolution in the mid-latitudes and $1^\circ \times 0.45^\circ$ longitude-latitude resolution in the tropics. There are 20 vertical levels with 15 m resolution near the sea surface. SODA is forced by monthly-mean wind stresses of the Comprehensive Ocean-Atmosphere Data Set (COADs) for the time period 1950–92. For 1992–2002, NCEP/NCAR reanalysis wind stress forcing is applied and satellite scatterometer winds are assimilated. SODA assimilates all types of available ocean observations, such as hydrography, XBTs, sea level and SST. Heat fluxes are estimated based on bulk formulae.

[7] SODA assimilation fields were earlier analyzed in comparison with other models and observations of the mean CEC [*Schott et al.*, 2002] and were also shown by *Xie et al.* [2002] to well represent the upper-layer and thermocline circulation of the subtropical South Indian Ocean. Furthermore, SODA transports of the Indonesian Throughflow (ITF) were found in agreement with observed transports [*England and Huang*, 2005].

3. Decadal Variability of the Cross-Equatorial Cell

3.1. Cross-Equatorial Sverdrup Transports

[8] Based on the above-described understanding of the mean CEC we first inspect the Sverdrup transports of the COADs wind stresses driving SODA. The Sverdrup transport time series, calculated from the stress curls at the equator (Figure 2a), has a southward mean of 5.4 ± 2.1 Sv for 1950–2001 and shows a steady decrease from the beginning in 1950 to the change in stresses applied to

[1]Leibniz-Institut für Meereswissenschaften an der Universität Kiel (IFM-GEOMAR), Kiel, Germany.

0094-8276/06/2006GL025891$05.00

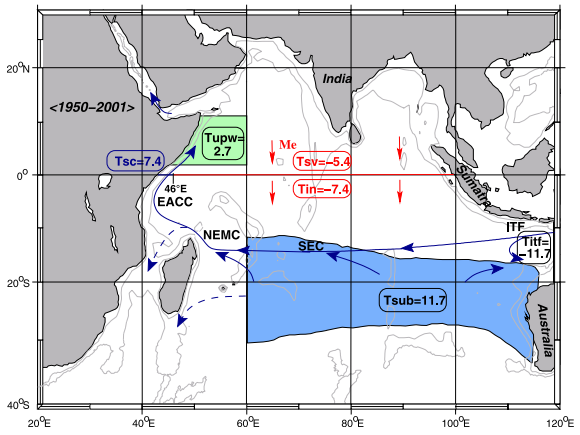

Figure 1. Schematic diagram of the mean circulation branches involved in the shallow Cross-Equatorial Cell (CEC) of the Indian Ocean, with SEC = South Equatorial Current, NEMC = Northeast Madagascar Current, EACC = East African Coast Current, Me = meridional Ekman transports and ITF = Indonesian Throughflow. Also shown are the areas for which upwelling off Africa and subduction in the southeastern subtropics were calculated from SODA. Mean transports for 1950–2001 (in Sv) are given for Sverdrup transport (T_{SV}), the upper Somali Current (T_{SC}), upwelling (T_{upw}), interior upper-layer return flow (T_{int}), subduction (T_{sub}) and ITF (T_{itf}); see text for details.

SODA in 1992. A line fit to the decreasing trend of southward Sverdrup transport yields 0.08 ± 0.01 Sv·yr^{-1} (Figure 2a). This trend implies a decrease of 3.2 Sv during the 40 year time period, more than half of the mean. Based on our reasoning for the mean CEC, this should imply a weakening of the shallow cross-equatorial overturning circulation.

3.2. Cross-Equatorial Exchange

[9] The cross-equatorial exchange is separately evaluated for the Somali Current region, west of 46°E and for the interior between 46°E and the eastern boundary. Profiles of the zonally (for the regions west and east of 46°E, respectively) and vertically (from the surface downward) integrated transports for 1950–2001 show the mean structure of the CEC (Figure 3a). In the interior, the southward transport mainly occurs in the top 60m, in accordance with the CEC mechanism, while in the Somali Current the northward transport occurs throughout the thermocline region. The net transport, integrated from coast to coast (Figure 3a) shows that the interior and Somali Current parts of the CEC cancel out at about the 340m depth level. The mean transports of the northward Somali Current and the southward interior cross-equatorial flow are 7.4 ± 4.0 Sv and −7.4 ± 2.6 Sv, respectively for the upper 340m (Figure 1). They are thus larger than the mean southward Sverdrup transport. The discrepancy has to do with a southward recirculation out of the Somali Current that returns at low latitudes before ever reaching the northern upwelling regimes and transports about 2 Sv southward between 46–49°E, putting the overall balance of Somali Current, interior southward flow and Sverdrup transport into good agreement with the CEC concept.

[10] The time series of the southward interior SODA transport, above 340m and integrated from 46°E to the eastern boundary (Figure 2b), shows a decreasing trend, of 0.09 ± 0.02 Sv·yr^{-1}, yielding a decrease of 3.6 Sv from 1950–91, similar to the decreasing trend of the Sverdrup transport slowdown that presumably drives it. The Somali Current transport anomaly time series for 1950–91 (Figure 2c) shows a somewhat larger decreasing trend, though with larger variability, of −0.12 ± 0.03 Sv·yr^{-1}.

[11] The difference of the CEC transport profiles (Figure 3b) between the first and the last decade of the trend fit time period shows that much of the transport difference is located in the thermocline; that is, the structure of the difference is not quite in agreement with a mere reduction of CEC intensity. As the x-z distribution of transport differences between the two decades shows (Figure 4), some thermocline recirculation occurs east of the Somali Current, as reported above for the mean, that is not part of the

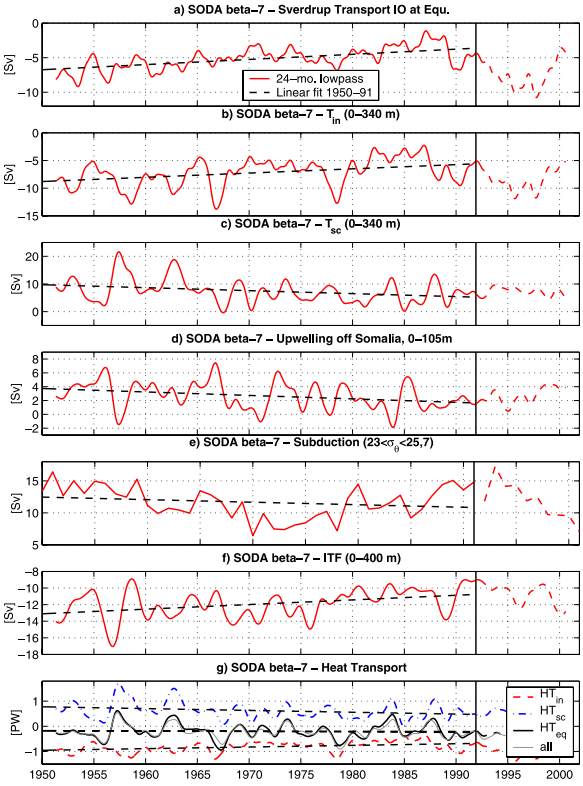

Figure 2. Variability 1950–2001 and trend fits 1950–91 of 24-month low-passed transport time series (in Sv) of CEC circulation elements in SODA: (a) cross-equatorial Sverdrup transports, from COADs wind stress curls; (b) interior transport in upper 340m (east of 46°E); (c) Somali Current transport in upper 340m; (d) upwelling off Somalia; (e) subduction in southeastern Indian Ocean; (f) Indonesian Throughflow (upper 400m); and (g) cross-equatorial heat transport (Somali Current to 340m, dash-dotted curve; interior to 340m, dashed curve; total section to 340m, thick black curve; total section to bottom, grey curve). Vertical line marks break in 1992 when SODA forcing switched from COADs wind stresses to NCEP forcing plus satellite scatterometry assimilation.

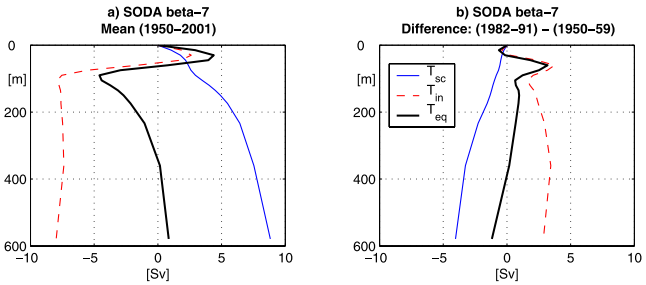

Figure 3. Meridional transports (Sv) across the equator from SODA: (a) mean zonal and vertical (from surface) integrals for Somali Current (west of 46°E, thin solid curve), interior (east of 46°E, dashed curve) and coast to coast (thick curve) for 1950–2001; (b) as in Figure 3a but for difference between decades 1982–91 and 1950–59.

meridional CEC and explains part of the transport decreasing trends of Figures 2b and 2c.

3.3. East African Upwelling and Southeastern Subduction

[12] Upwelling returns thermocline water to the surface as part of the CEC. The main northern Indian Ocean upwelling region is located off East Africa, others are off the Arabian Peninsula and in domes east and West of India and Sri Lanka [*Miyama et al.*, 2003; *Schott et al.*, 2002]. The mean upwelling off northeast Africa in SODA, calculated across the 105m depth level for the area marked in Figure 1, amounts to 2.7 ± 1.8 Sv. The upwelling time series (Figure 2d) also shows a decreasing trend, of −0.06 ± 0.01 Sv·yr^{-1}, yielding a decrease of 2.4 Sv over the four decades of the trend.

[13] Subduction supplies the downward branch of the CEC south of the equator and occurs in the southeastern subtropical Indian Ocean [*Karstensen and Quadfasel*, 2002]. Subduction transport was calculated for the area marked in Figure 1, following *Marshall et al.* [1993]. The calculation evaluated the Ekman pumping and lateral induction terms from the SODA wind stresses, density and velocity fields. The mean obtained for the subduction region of Figure 1 was 11.7 ± 2.6Sv into the density range σ_θ = 23.0–25.7 kgm^{-3} that can contribute to northern upwelling. Subduction was also showing a decreasing trend, of −0.04 ± 0.06 Sv·yr^{-1} over the 1950–91 time period (Figure 2e), although superimposed by a larger multidecadal variation with a minimum during 1970–78, the reason for the large standard deviation of the trend slope.

3.4. Indonesian Throughflow

[14] The Indonesian Throughflow (ITF) spreads zonally toward Madagascar, and much of it appears to supply the southward transport through the Mozambique Channel in SODA. It is not clear from observations how the ITF contributes to the CEC, but model particle studies [*Miyama et al.*, 2003] have traced upwelling waters in the northern Indian Ocean upwelling sites back to the Indonesian passages and western Pacific. Its top-to bottom mean is 16.3 Sv, but for our CEC discussion only the upper 400m are relevant, for which the mean ITF is 11.7 ± 1.7 Sv (Figure 1). The transport time series for the upper 400m (Figure 2f) shows a decreasing trend of 0.06 ± 0.01 Sv.

3.5. Cross-Equatorial Heat Transport

[15] With the mean cross-equatorial transport closed for the upper 340m (Figure 3a), heat transport can be calculated for this layer, yielding −0.23 ± 0.29 PW, very close to the section total of −0.24 ± 0.24 PW. The mean southward heat export across the equator is due to the excess of the southward interior heat transport of −0.83PW over the northward heat transport of 0.60 PW by the Somali Current. However, for the variability the interesting result is that the changing contributions of the Somali Current (Figure 2g, dash-dotted curve) and of the southward interior flow (Figure 2g, dashed curve) about compensate each other, yielding no trend, neither for the top 340m (Figure 2g, thick black curve) nor for the section total (Figure 2g, light grey curve).

[16] The transport-weighted mean temperatures of the Somali Current and interior upper-layer flow, respectively, do not show any trends, confirming that the heat transport changes of Figure 2g are solely due to the volume transport changes involved. The heat storage for the northern Indian Ocean (not shown) does not show any trend, either. Due to the fact that the "optimum interpolation" method used in the SODA assimilation generates interior heat sources and sinks to fit the model temperatures to the observations and that these data are not available, we did not determine a box heat budget for the northern Indian Ocean.

4. Conclusions

[17] While for the rather well observed Tropical Pacific [*McPhaden and Zhang*, 2002] and even Atlantic [*Schott et al.*, 2004] observations are now available that allow the analysis of the means and variability of the Subtropical Cells, or at least of some of their branches, nothing is really known from observations on the variations of the Cross-equatorial Cell (CEC) of the Indian Ocean. We have analyzed the output fields of the SODA beta-7 assimilation for the time period 1950–2001, and find for the mean circulation of the CEC in SODA that its structure and transports (Figures 1 and 3) agree well with corresponding observational results [*Schott et al.*, 2002].

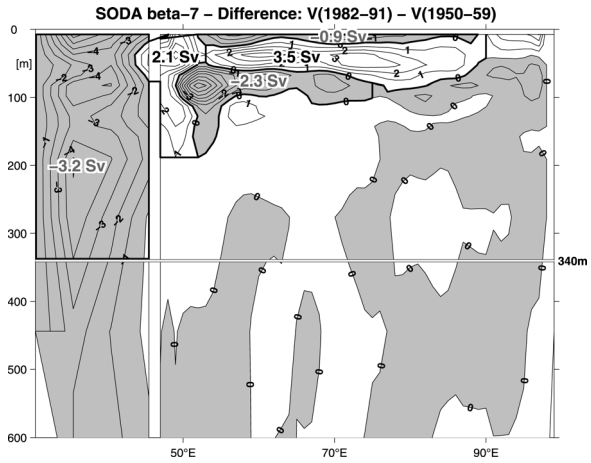

Figure 4. Difference of meridional currents and transports (in marked boxes) between the periods 1982–91 minus 1950–59 for the upper 600m along the equator; southward flow anomalies grey-shaded.

[18] SODA circulation variability shows drastic changes after the SODA wind stress forcing was changed from COADs wind stresses to NCEP/NCAR reanalysis wind stresses and scatterometer assimilation in 1992 (Figure 2). Analysis of the variability of the cross-equatorial exchange for the pre-satellite era reveals that during the first four decades of the SODA assimilation, 1950–91, significant multidecadal changes occurred in practically all elements that participate in the Indian Ocean cross-equatorial cell (CEC):

[19] • The southward cross-equatorial Sverdrup transport (Figure 2a) that drives the CEC is reduced by about half its mean. In agreement with the reduced driving, both the southward interior upper-layer flow (Figure 2b) and the Somali Current thermocline flow (Figure 2c) decrease. After reduction by the fraction of this decrease that is due to Somali Current recirculation (Figure 4), the net slow-down of the CEC is in agreement with the reduction of the cross-equatorial Sverdrup transport.

[20] • Other elements that participate in the CEC are also showing a reduction over the four decades of our trend analysis: Northern upwelling, off Somalia, is substantially reduced (Figure 2d) and there is also a downward trend in southeastern subtropical subduction (Figure 2e), although subduction shows a different type of decadal variability than the other CEC elements. In addition, the upper-layer (0–400m) Indonesian Throughflow shows a decreasing trend, resulting in a reduction by 2.4 Sv over the four decades (Figure 2f).

[21] • The heat transport time series of the upper 340m (which has zero mean mass transport balance, Figure 3a), well represents total cross-equatorial heat transport variability (Figure 2g). The effect of the CEC slowdown on the cross-equatorial heat transport is small, since the reductions in both components, Somali Current and interior, about cancel each other. The approximate constancy of the cross-equatorial heat export during 1950–90 may be considered in agreement with the constant heat storage found for SODA in the Indian Ocean north of the equator. On the other hand, evaluation of the northern Indian Ocean heat budget would have required knowledge of the heat storage changes caused by the "optimum interpolation" method applied in SODA assimilation procedure, but these terms were not available.

[22] While it is obvious that for the early part of the SODA assimilation only few data are available for constraining the solution, the mechanisms of the combined changes that SODA displays help to better understand the potential mechanisms of longer-period variability in the Indian Ocean. With the cross-equatorial Sverdrup transport being the driver of the demonstrated CEC slowdown in this study, it will be interesting to investigate the CEC variability in other decadal model simulations and assimilation, with other wind forcing and possibly other assimilation methods. For example, the cross-equatorial Sverdrup transports based on ERA-40 wind stresses also show a decadal decrease, though weaker than in Figure 2a, while no such decreasing decadal trend is apparent in NCEP based Sverdrup transports.

[23] **Acknowledgments.** This study was supported by the German CLIVAR/marin Program, contract 03F0377B, and by Deutsche Forschungsgemeinschaft (DFG), contract Scho 168/29-2. We thank Rainer Zantopp of IFM-GEOMAR for his help in the data analysis.

References

Carton, J. A., G. Chepurin, X. Cao, and B. Giese (2000), A simple ocean data assimilation analysis of the global upper ocean 1950–1995. part I: Methodology, *J. Phys. Oceanogr.*, *30*, 294–309.

England, M. H., and F. Huang (2005), On the interannual variability of the Indonesian Throughflow and its linkage with ENSO, *J. Clim.*, *18*, 1435–1444.

Godfrey, J. S., G. C. Johnson, M. J. McPhaden, G. Reverdin, and S. Wijffels (2001), The tropical ocean circulation, in *Ocean Circulation and Climate*, edited by J. Church, J. Gould, and G. Siedler, pp. 215–245, Elsevier, New York.

Karstensen, J., and D. Quadfasel (2002), Formation of Southern Hemisphere thermocline waters: Water mass conversion and subduction, *J. Phys. Oceanogr.*, *32*, 3020–3038.

Lee, T. (2004), Decadal weakening of the shallow overturning circulation in the South Indian Ocean, *Geophys. Res. Lett.*, *31*, L18305, doi:10.1029/2004GL020884.

Marshall, J. C., A. J. G. Nurser, and R. G. Williams (1993), Inferring the subduction rate and period over the North Atlantic, *J. Phys. Oceanogr.*, *23*, 1315–1329.

McPhaden, M. J., and D. Zhang (2002), Slowdown of the meridional overturning circulation in the upper Pacific Ocean, *Nature*, *415*, 603–608.

Miyama, T., J. P. McCreary Jr., T. G. Jensen, J. Loschnigg, S. Godfrey, and A. Ishida (2003), Structure and dynamics of the Indian-Ocean cross-equatorial cell, *Deep Sea Res., Part II*, *50*, 2023–2047.

Schott, F., and J. P. McCreary (2001), The monsoon circulation of the Indian Ocean, *Progr. Oceanogr.*, *51*, 1–123.

Schott, F. A., M. Dengler, and R. Schoenefeldt (2002), The shallow overturning circulation of the Indian Ocean, *Progr. Oceanogr.*, *52*, 57–1003.

Schott, F. A., J. P. McCreary, and G. C. Johnson (2004), Shallow overturning circulations of the tropical-subtropical oceans, in *Earth's Climate: The Ocean-Atmosphere Interaction*, *Geophys. Monogr. Series.*, vol. 147, edited by C. Wang, S.-P. Xie, and J. A. Carton, pp. 261–304, AGU, Washington, D. C.

Wacongne, S., and R. Pacanowski (1996), Seasonal heat transport in a primitive equations model of the tropical Indian Ocean, *J. Phys. Oceanogr.*, *26*, 2666–2699.

Xie, S.-P., H. Annamalai, F. Schott, and J. P. McCreary Jr. (2002), Origin and predictability of South Indian Ocean climate variability, *J. Clim.*, *15*, 864–874.

R. Schoenefeldt and F. A. Schott, IFM-GEOMAR, Düsternbrooker Weg 20, D-24105 Kiel, Germany. (fschott@ifm-geomar.de)